Theoretical Studies of *o*-, *m*-, and *p*-Benzyne Negative Ions

John J. Nash and Robert R. Squires*

Contribution from the Department of Chemistry, Purdue University, West Lafayette, Indiana 47907

Received February 29, 1996. Revised Manuscript Received May 28, 1996[⊗]

Abstract: A general theoretical description of "distonic" radical anions is presented, along with an account of an extensive series of *ab initio* molecular orbital and density functional theory calculations on the negative ions of *o*-, *m*- and *p*-benzyne. The performance of several different computational methods is evaluated with respect to artifactual symmetry-breaking. QCISD(T), CCSD(T), CASPT2N, and DFT(B3LYP) calculations employing double-ζ quality basis sets predict that *o*-, *m*-, and *p*-benzyne anions all have high-symmetry, delocalized radical anion ground electronic states: $^2B_2$ (C_{2v}), $^2B_2$ (C_{2v}), and ^2A_g (D_{2h}), respectively. The *meta* and *para* isomers also exhibit low-lying, localized radical anion forms with distorted geometries that arise by pseudo Jahn-Teller interactions (vibronic coupling): $^2A'$ (C_s) for *m*-benzyne anion and $^2A_1$ (C_{2v}) for *p*-benzyne anion. Broken-symmetry wave functions are obtained at symmetrical geometries from MCSCF and CISD calculations for *p*-benzyne anion, but not for *o*- and *m*-benzyne anions. The calculated potential energy surfaces for in-plane distortion of *m*- and *p*-benzyne anions are found to be quite flat. An isodesmic reaction approach is used to calculate the electron, proton, and hydrogen atom-binding energies for each of the minimum energy states. Good agreement is achieved between the experimental estimates for these quantities and the calculated values for the lowest-energy anion states. The implications of the theoretical findings for negative ion photoelectron spectroscopic measurements with the *m*- and *p*-benzyne anions are discussed.

Introduction

In the preceding paper,[1] we described a gas-phase experimental investigation of the formation, structures, and thermochemical properties of the benzyne negative ions, **1a**−**3a**. The

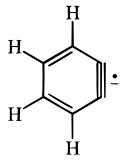

1a

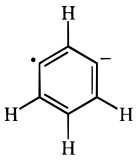

2a

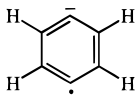

3a

meta and *para* isomers were previously unknown. Their rational synthesis and identification is important because these species are required for negative ion photoelectron spectroscopic measurements[2] of the singlet−triplet splittings and electron affinities of the corresponding neutral biradicals *m*-benzyne (**2**) and *p*-benzyne (**3**). From a more general perspective, the benzyne anions comprise an interesting series of "distonic radical ions",[3] wherein the positions of the formally charged and odd-spin sites in each isomer differ in a well-defined manner. Also, the benzyne anions are isoelectronic with the positively-charged molecular ions of the diazabenzenes pyridazine, pyrimidine and pyrazine, and they are closely related to the nπ* excited states of these molecules. The diazabenzenes have been the subjects of numerous spectroscopic[4] and theoretical[5] investigations of lone pair interactions and vibronic coupling in organic molecules, and many of the physical insights obtained from these studies are directly applicable to the benzyne anions. In this paper we describe an extensive series of *ab initio* molecular orbital calculations on the benzyne anions, which were carried out in order to acquire a basic understanding of their electronic structures and physical properties and to obtain theoretical data that may aid in the interpretation of the photoelectron spectra that are ultimately obtained for the *meta* and *para* isomers. A general theoretical description of "distonic" radical anions is presented, along with a detailing of the computational results for the benzyne anions.

Distonic Radical Anions: General Considerations

The term "distonic ion", as originally coined by Radom and co-workers,[3] refers to an ion with formally separated charge and radical sites. Distonic ions may be divided into two distinct classes, depending upon the nature of the charged site. The most commonly studied form of distonic ion possesses a coordinatively- and electronically-saturated charged site (usually of the onium type), such as in the so-called "ylidions" (ionized ylides) and their homologs. The other type of distonic ion corresponds to an ionized biradical or zwitterion,[3] which possesses two coordinatively-unsaturated sites containing one or three electrons. An important consequence of this latter topology is the possibility for *at least two* low-lying electronic states of the distonic ion, wherein the odd electron occupies one or the other of the two nominally nonbonding orbitals.

[⊗] Abstract published in *Advance ACS Abstracts,* November 1, 1996.

(1) Wenthold, P. G.; Hu, J.; Squires, R. R. *J. Am. Chem. Soc.* **1996**, *118*, 11865.

(2) Ervin, K. M.; Lineberger, W. C. In *Advances in Gas Phase Ion Chemistry*; Adams, N. G., Babcock, L. M., Eds.; JAI Press: Greenwich, CT, 1992; Vol. 1.

(3) (a) Yates, B. F.; Bouma, W. J.; Radom, L. *J. Am. Chem. Soc.* **1984**, *106*, 5805. (b) Yates, B. F.; Bouma, W. J.; Radom, L. *Tetrahedron* **1986**, *42*, 6225. (c) Hammerum, S. *Mass Spectrom. Rev.* **1988**, *7*, 123.

(4) (a) Innes, K. K.; Ross, I. G.; Moomaw, W. R. *J. Mol. Spectrosc.* **1988**, *132*, 492. (b) Walker, I. C.; Palmer, M. H. *Chem. Phys.* **1991**, *153*, 169; **1991**, *157*, 187. (c) Bolovinos, A.; Tsekeris, P.; Philis, J.; Pantos, E.; Andritsopoulus, G. *J. Mol. Spectrosc.* **1984**, *103*, 240.

(5) (a) Wadt, W. R.; Goddard, W. A. *J. Am. Chem. Soc.* **1975**, *97*, 2034. (b) Kleier, D. A.; Martin, R. L.; Wadt, W. R.; Moomaw, W. R. *J. Am. Chem. Soc.* **1982**, *104*, 60. (c) Ellenbogen, J. C.; Feller, D.; Davidson, E. R. *J. Phys. Chem.* **1982**, *86*, 1583. (d) Fülscher, M. P.; Anderssom, K; Roos, B. O. *J. Phys. Chem.* **1992**, *96*, 9204. (e) Zeng, J.; Hush, N. S.; Reimers, J. R. *J. Chem. Phys.* **1993**, *99*, 1495; 1508. (f) Woywod, C.; Domcke, W.; Sobolewski, A. L.; Werner, H.-J. *J. Chem. Phys.* **1994**, *100*, 1400. (g) Zeng, J.; Woywod, C.; Hush, N. S.; Reimers, J. R. *J. Am. Chem. Soc.* **1995**, *117*, 8618.

S0002-7863(96)00664-6 CCC: $12.00

Inasmuch as the benzyne anions belong to this particular class of distonic ion, we can anticipate the existence of multiple low-lying electronic states for these species. However, organic anions with *bound* electronically-excited states are a rarity, since the excitation energies usually exceed the electron affinities of the corresponding neutral molecules.[6] In order to put these ideas in perspective and apply them to the benzyne anions, we must first develop a general picture of biradical negative ions in terms of the symmetry properties of their neutral biradical precursors.

Salem and Rowland[7] define a biradical as a molecule possessing two weakly interacting electrons in degenerate or nearly degenerate molecular orbitals.[8] These molecular orbitals are constituted from the two localized nonbonding orbitals, n_1 and n_2, and their electronic interaction may result from direct (through-space) overlap or indirect (through-bond)[9] coupling between n_1 and n_2 or from electron exchange:

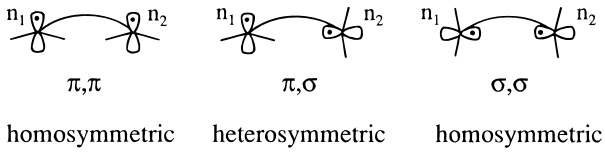

It is useful to classify biradicals (and ionized biradicals) according to the topological relationship between the two nonbonding orbitals.[7] As illustrated above, a *homosymmetric* biradical is characterized by a symmetry element, such as a reflection plane or a proper rotation axis, which relates n_1 to n_2 and allows them to mix, while in a *heterosymmetric* biradical n_1 and n_2 belong to different symmetry representations and, therefore, do not mix. A *nonsymmetric* biradical represents the intermediate case in which there are no symmetry constraints on the mixing between n_1 and n_2.

The benzynes, **1**−**3**, are homosymmetric biradicals of the (σ,σ) type, wherein n_1 and n_2 are related by a plane and one or two C_2 axes.[10] The molecular orbitals for homosymmetric biradicals are given by the symmetric and antisymmetric combinations of n_1 and n_2: $\Psi_+ = (n_1 + n_2)$ and $\Psi_- = (n_1 - n_2)$. As shown in Figure 1, in *o*- and *m*-benzyne Ψ_+ lies energetically below Ψ_- due to direct overlap between n_1 and n_2, while in *p*-benzyne "through-bond coupling" [9] involving the intervening CC bonds places Ψ_- below Ψ_+. The orbital splittings naturally decrease as the magnitude of the interaction between n_1 and n_2 decreases. For example, ROHF/6-31G(d) calculations[10k] on the triplet states of *o*-, *m*- and *p*-benzyne give $|\Psi_- - \Psi_+|$ orbital energy gaps of 40, 33, and 11 kcal/mol, respectively. The relatively large orbital splittings in the benzynes lead to singlet ground states for all three isomers. It is well-known that the totally-symmetric singlet states of homosymmetric biradicals require a minimal two-configuration representation.[7,8] The singlet ground states of the benzynes can be described by the simplified two-configuration wave function shown below with CI coefficients c_1 and c_2

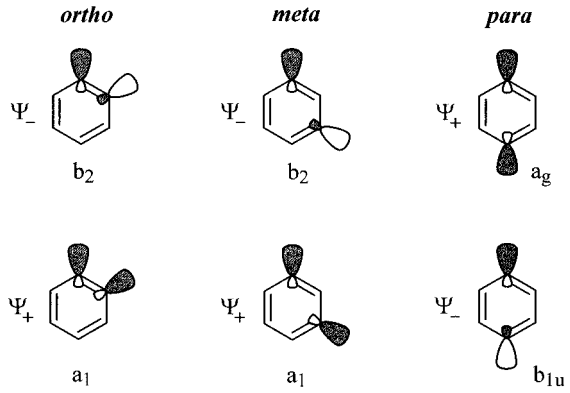

Figure 1. Schematic representations of the highest-occupied and lowest-unoccupied molecular orbitals of *o*-, *m*- and *p*-benzyne, **1**−**3**.

$$^1\Psi = (c_1^2 + c_2^2)^{-1/2}[c_1\Psi_+^2 - c_2\Psi_-^2](\alpha\beta - \beta\alpha) \quad (1)$$

Values for (c_1, c_2) obtained from MCSCF calculations carried out in our previous theoretical study[10k] are (0.898, −0.255), (0.846, −0.398), and (−0.566, 0.731) for the $^1A_1$, $^1A_1$, and ^1A_g ground states of *o*-, *m*-, and *p*-benzyne, respectively. Inasmuch as $c_1^2 = c_2^2$ for a "pure" biradical, the computed values for the benzynes indicate that the *para* isomer has the greatest biradical character, while the *ortho* isomer has the least.

Occupation of the two valence orbitals Ψ_+ and Ψ_- by three electrons gives rise to a pair of radical anion doublet *electronic states*[11] with the nominal configurations $\Psi_+^2\Psi_-^1$ and $\Psi_+^1\Psi_-^2$ (Figure 2). A two-configuration representation is no longer required since the overall symmetry of each doublet configuration is determined by that of the singly-occupied orbital, and Ψ_+ and Ψ_- will always belong to different symmetry representations. These two distonic ion doublet electronic states will have the same molecular symmetry as that of the homosymmetric biradical from which they are derived, and will possess equal odd-spin and negative charge density at both sites, i.e., they are "delocalized" states (Figure 2a). However, there are additional possibilities to consider. Depending upon the magnitude of the $|\Psi_- - \Psi_+|$ orbital energy gap, a distonic anion derived from a homosymmetric biradical may be subject to the pseudo Jahn-Teller effect[12,13] wherein the $\Psi_+^2\Psi_-^1$ and

(6) Drzaic, P.; Marks, J.; Brauman, J. I. In *Gas Phase Ion Chemistry*; Bowers, M. T., Ed.; Academic Press: New York, 1984; Vol. 3, Chapter 21.

(7) Salem, L.,; Rowland, C. *Angew. Chem., Int. Ed. Engl.* **1972**, *11*, 92.

(8) Additional general discussions of biradicals may be found: (a) Michl, J. *Mol. Photochem.* **1972**, *4*, 257; Bonačić-Koutecký, V.; Koutecký, J.; Michl, J. *Angew. Chem., Int. Ed. Engl.* **1987**, *26*, 170. (b) *Diradicals* Borden, W. T., Ed.; Wiley: New York, 1982.

(9) (a) Hoffmann, R.; Imamura, A.; Hehre, W. J. *J. Am. Chem. Soc*. **1968**, *90*, 1499. (b) Hoffmann, R. *Acc. Chem. Res.* **1971**, *4*, 1. (c) Gleiter, R. *Angew. Chem., Int. Ed. Engl.* **1974**, *13*, 696. (d) Paddon-Row, M. N. *Acc. Chem. Res.* **1982**, *15*, 245. (e) Goldberg, A. H.; Dougherty, D. A. *J. Am. Chem. Soc.* **1983**, *105*, 284. (f) Paddon-Row, M. N.; Jordan, K. D. *J. Am. Chem. Soc.* **1993**, *115*, 2952.

(10) (a) Wilhite, D. L.; Whitten, J. L. *J. Am. Chem. Soc*. **1971**, *93*, 2858. (b) Dewar, M. J. S.; Li, W.-K. *J. Am. Chem. Soc*. **1974**, *96*, 5569. (c) Dewar, M. J. S.; Ford, G. P.; Reynolds, C. H. *J. Am. Chem. Soc*. **1983**, *105*, 3162. (d) Noell, J. O.; Newton, M. D. *J. Am. Chem. Soc*. **1979**, *101*, 51. (e) Radom, L.; Nobes, R. H.; Underwood, D. J.; Wai-Kee, L. *Pure Appl. Chem.* **1986**, *58*, 75. (f) Rigby, K.; Hillier, I. H.; Vincent, M. *J. Chem. Soc., Perkin Trans II* **1987**, 117; Hillier, I. H.; Vincent, M. A.; Guest, M. F.; Von Niessen, W. *Chem. Phys. Lett*. **1987**, *134*, 403. (g) Scheiner, A. C.; Schaefer, H. F. III; Liu, B. *J. Am. Chem. Soc*. **1989**, *111*, 3118; Scheiner, A. C.; Schaefer, H. F. III *Chem. Phys. Lett*. **1991**, *177*, 471. (h) Liu, R.; Xuefeng, Z.; Pulay, P. *J. Phys. Chem*. **1992**, *96*, 8336. (i) Sutter, H. U.; Ha, T.-K. *Chem. Phys. Lett*. **1992**, *198*, 259. (j) Nicolaides, A.; Borden, W. T. *J. Am. Chem. Soc.* **1993**, *115*, 11951. (k) Wiershke, S. G.; Nash, J. J.; Squires, R. R. *J. Am. Chem. Soc.* **1993**, *115*, 11958. (l) Karadahov, P. B.; Gerratt, J.; Raos, G.; Cooper, D. L.; Raimondi, M. *Isr. J. Chem.* **1993**, *33*, 253. (m) Kraka, E.; Cremer, D. *Chem. Phys. Lett.* **1993**, *216*, 333. Kraka, E.; Cremer, D. *J. Am. Chem. Soc.* **1994**, *116*, 4936. (n) Lindh, R.; Persson, B. J. *J. Am. Chem. Soc.* **1994**, *116*, 4963. Lindh, R.; Lee, T. J.; Bernhardsson, A.; Persson, B. J.; Karlström, G. *J. Am. Chem. Soc.* **1995**, *117*, 7186.

(11) In this paper we take pains to qualify the term "state". The "electronic states" calculated by the quantum mechanical procedures discussed in the text represent a motionless nuclear configuration with a defined electronic configuration (or mixture of configurations), corresponding to a single stationary point on the potential energy surface. A complete "state" of a molecule, such as one observes in a spectroscopic experiment, includes a wave function for the nuclei and possesses zero-point motion that may encompass many different stationary points on the global potential energy surface, with dynamic coupling between the nuclear and electronic degrees of freedom.

(12) (a) Öpik, U.; Pryce, M. L. H., *Proc. Roy. Soc. (London)* **1957**, *A238*, 425. (b) Bader, R. F. W. *Can. J. Chem.* **1962**, *40*, 1164. (c) Pearson, R. G. *J. Am. Chem. Soc.* **1969**, *91*, 4947.

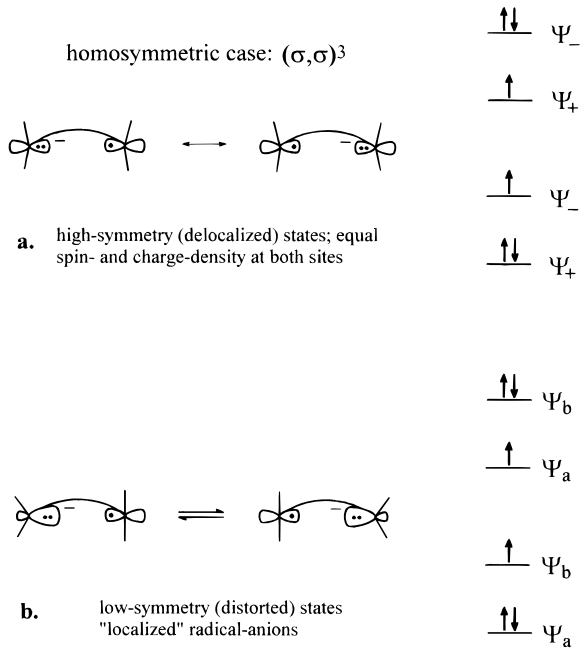

Figure 2. Electronic structure model for a distonic radical anion derived from a homosymmetric (σ,σ) biradical: a. Spin- and charge-delocalized states with the same molecular symmetry as the neutral biradical. b. Pseudo Jahn-Teller (vibronic) interactions lead to "localized" radical anion states with reduced molecular symmetry.

$\Psi_+{}^1\Psi_-{}^2$ configurations are mixed by a molecular distortion. This vibronic coupling can lead to new stationary points (minima) on the potential energy surface with reduced molecular symmetry. The electronic character of these reduced-symmetry stationary points is that of a "localized" distonic radical anion, with the negative charge and odd-spin density largely constrained to separate sites (Figure 2b). The lower energy delocalized electronic state (e.g., $\Psi_+{}^2\Psi_-{}^1$) will be either the global minimum or a transition state between equivalent distorted minima on the resulting "double-cone" potential energy surface.[13] If the barrier between the distorted minima is below the zero-point energy level for the distortion, then the lowest *vibronic state*[11] of the radical ion will be fluxional with respect to the different geometric forms. If the barrier lies well-above the zero-point level, then discrete, low-symmetry states can be observed.

However, one must exercise caution in evaluating the significance of calculated structures for open-shell species of reduced symmetry because of the well-known "doublet instability" problem[14] that can afflict molecular orbital calculations on delocalized radicals, radical ions, and biradicals.[15] For three-center systems such as allyl radical or NO_2, doublet instability arises from insufficient correlation between the open-shell electron and the electrons in the next lower-lying orbital. Broken-symmetry solutions to the Hartree−Fock equations for delocalized radicals with otherwise symmetrical structures can arise as an artifact of the inadequacies of a single-configuration representation. Localization of the unpaired electron results as the system acts to minimize Coulombic repulsion between this electron and the electron of opposite spin in the immediately subjacent orbital that spans the same atoms as the singly-occupied orbital. In unconstrained geometry optimizations, doublet instability can spuriously result in unsymmetrical, localized structures as low-lying or global minima, and the problem can be aggravated by the use of small basis sets. The same types of unsymmetrical structures that are produced by the *real* effects of pseudo Jahn-Teller interactions can also arise as artifacts of doublet instability. Doublet instability can in some cases be remedied by providing different spatial wave functions for electrons of opposite spin, as in the unrestricted Hartree−Fock (UHF) approach, or by employing MCSCF or CI procedures that allow correlation of the unpaired electron with electrons in the subjacent orbital.

Nevertheless, for some systems artifactual symmetry-breaking can persist even at MCSCF and CI levels of theory.[16] Broken-symmetry multiconfigurational or limited CI wave functions can sometimes result for symmetrical geometries when dynamic correlation between the electrons in the σ and π molecular orbitals is not adequately represented in the MCSCF or CI expansions. This produces a cusp on the potential energy surface at the symmetrical geometry that leads to a discontinuous change in the energy with small symmetry-breaking molecular distortions. Therefore, an unconstrained geometry optimization will erroneously lead to a minimum with a distorted structure. These effects are especially problematic in calculations on charged or heteropolar open-shell systems[15−19] and in calculations on systems possessing equivalent, weakly-interacting pairs of orbitals containing one or three electrons.[5,20] This problem is therefore endemic to calculations involving distonic radical ions derived from biradicals.

Benzyne Anions

For C_{2v} *o*- and *m*-benzyne, the biradical molecular orbitals, Ψ_+ and Ψ_-, are of a_1 and b_2 symmetry, respectively, while for D_{2h} *p*-benzyne they are of a_g and b_{1u} symmetry (Figure 1). Therefore, the two high-symmetry, delocalized electronic states for *o*-benzyne anion (**1a**) and *m*-benzyne anion (**2a**) will have the configurations $[a_1{}^2b_2{}^1]$, corresponding to the lower energy $^2B_2$ electronic state, and $[a_1{}^1b_2{}^2]$, corresponding to the higher energy $^2A_1$ electronic state. For *p*-benzyne, the ^2A_g electronic state ($[b_{1u}{}^2a_g{}^1]$ occupation) will lie energetically below the $^2B_{1u}$ electronic state ($[b_{1u}{}^1a_g{}^2]$ occupation). These delocalized configurations are illustrated in the upper portion of Figure 3. The two configurations can be mixed in each benzyne anion by a molecular distortion, provided the energy difference between them is sufficiently small and a normal mode exists in the molecule with the same symmetry as the product of the symmetries of the two configurations, i.e., by pseudo Jahn-Teller interactions.[12,13] For both **1a** and **2a**, a b_2 mode distorts the ions to C_s structures ($^2A'$ electronic states) by increasing the CCC angle about one dehydrocarbon and decreasing the CCC angle about the other. For **3a**, an analogous molecular distortion from D_{2h} to C_{2v} symmetry occurs by a b_{1u} mode to produce a pair of $^2A_1$ electronic states.[21] The angular distortions accompanying pseudo Jahn-Teller interactions between the two configurations are exactly what one expects for "localization" of the odd-spin and negative charge densities in a benzyne radical anion since, compared to benzene, phenyl anion exhibits

(13) Bersuker, I. B. *The Jahn-Teller Effect and Vibronic Interactions in Modern Chemistry*; Plenum Press: New York, 1984.
(14) (a) Paldus, J.; Veillard, A. *Mol. Phys.* **1978**, *35*, 445. (b) Huyser, E. S.; Feller, D.; Borden, W. T.; Davidson, E. R. *J. Am. Chem. Soc.* **1982**, *104*, 2956.
(15) Borden, W. T.; Davidson, E. R.; Feller, D. *Tetrahedron* **1982**, *38*, 737.
(16) Davidson, E. R.; Borden, W. T. *J. Phys. Chem.* **1983**, *87*, 4783.
(17) Feller, D.; Davidson, E. R.; Borden, W. T. *J. Am. Chem. Soc.* **1984**, *106*, 2513.
(18) (a) Feller, D.; Huyser, E. S.; Borden, W. T.; Davidson, E. R. *J. Am. Chem. Soc.* **1983**, *105*, 1459. (b) McLean, A. D.; Lengsfield, B. H.; Pacansky, J.; Ellinger, Y. *J. Chem. Phys.* **1985**, *83*, 3567. (c) Rauk, A.; Yu, D.; Armstrong, D. A.; *J. Am. Chem. Soc.* **1994**, *116*, 8222.
(19) Borden, W. T.; Davidson, E. R.; Feller, D. *J. Am. Chem. Soc.* **1980**, *102*, 5302; **1981**, *103*, 5725.
(20) Borden, W. T.; Davidson, E. R. *Acc. Chem. Res.* **1996**, *29*, 67.

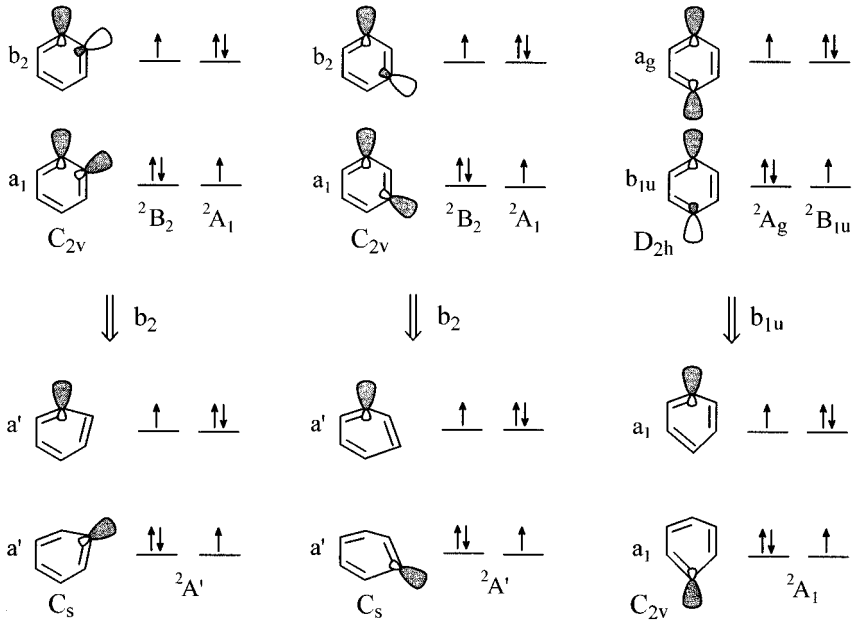

Figure 3. Schematic representations of the valence orbitals, electron occupations and state symmetries for the delocalized and localized forms of *o*-, *m*- and *p*-benzyne anions, **1a**−**3a**. The symmetry of the vibronic mode leading to the molecular distortion is also indicated.

a relatively small CCC angle (111°), while in phenyl radical it is relatively large (124°).[22] These localized configurations are schematically illustrated in the lower portion of Figure 3. Out-of-plane deformations of the benzyne anions are also conceivable which would, for example, reduce the symmetry of **3a** from D_{2h} to C_{2h} via a molecular distortion of either b_{1g} or b_{2g} symmetry. However, out-of-plane distortion requires interaction of the ground states of the benzyne anions with relatively high-lying πn and nπ^* excited states, so this mode of vibronic coupling should be relatively weak. The calculations described in the next section confirm this expectation.

The influence of vibronic coupling in the measured photoelectron and electronic spectra of diazabenzenes, and the manifold problems associated with artifactual symmetry-breaking in calculations on these molecules have been extensively documented.[4,5,23,24] The nπ^* excited states of pyrimidine (1,3-diazabenzene) and pyrazine (1,4-diazabenzene) are neutral analogs of *m*- and *p*-benzyne anions, respectively, in that each possesses three electrons in two weakly-interacting sigma orbitals. High-symmetry structures, with the excitation delocalized between equivalent nitrogens, are indicated by high resolution spectroscopic data[4] and by multireference CI calculations including dynamic electron correlation.[5e−g] However, the computed potential energy surfaces for both in-plane and out-of-plane distortions of these excited states are extremely flat, and the observed excitation spectra are indicative of extensive vibronic activity involving the low-lying $\pi\pi^*$ states.

Results

Ab initio molecular orbital calculations were carried out on the low-lying electronic states of *o*-, *m*-, and *p*-benzyne negative ions using multiconfigurational SCF and CI procedures that are analogous to those employed in our previous theoretical studies of the neutral benzynes[10k] and the α,n-dehydrotoluenes.[25] In addition, because of the challenges noted above that are associated with artifactual symmetry-breaking in calculations on distonic radical ions, some additional theoretical methods were employed that include more complete $\sigma-\pi$ electron correlation. The performance of density functional theory (DFT)[26] was also evaluated. Pairs of high-symmetry, delocalized electronic states have been located for all three benzyne anion isomers, while only the *meta* and *para* isomers were found to exhibit reduced-symmetry, localized radical anion structures as low energy forms. Calculations of the geometries and energies of these species are described below. Estimates of the electron, proton, and hydrogen atom binding energies of each benzyne anion have been derived for comparison with the experimentally-determined values.[1]

Geometries and Vibrational Frequencies. Pilot calculations on the low-lying electronic states of **1a**, **2a**, and **3a** were carried out at the ROHF level using the 6-31G(d) basis set.[27] Optimization of the geometries of **1a** and **2a** within C_s symmetry and **3a** within C_{2v} symmetry gave low-symmetry, localized radical anion structures for all three isomers: ^{2}A′ electronic states for **1a** and **2a** and the $^2A_1$ electronic state for **3a**. However, because of the restricted nature of the calculations, these results are likely to be an artifact of the symmetry-breaking problem described in the previous section. Accordingly, additional calculations were carried out using a MCSCF procedure and the 3-21G basis set.[27] For these calculations, nine active electrons were distributed among all symmetry-allowed configurations involving the two nonbonding σ orbitals and the six π and π^* orbitals (designated MCSCF(9,8)/3-21G).

(21) Actually, the pseudo Jahn-Teller interactions produce two different ^{2}A′ electronic states for **1a** and **2a**, and two different $^2A_1$ electronic states for **3a**, corresponding to the two possible occupations of each pair of localized orbitals that result from the vibronic mixing (a′ for **1a** and **2a**, and a_1 for **3a**). The higher-energy ^{2}A′ and $^2A_1$ electronic states correspond to the inner "cones" of the double-cone potential energy surfaces, and they possess symmetrical minimum-energy structures intermediate between those of the two delocalized electronic states.

(22) Gunion, R.; Gilles, M. K.; Polak, M.; Lineberger, W. C. *Int. J. Mass Spectrom. Ion Processes* **1992**, *117*, 601.

(23) Zhu, L.; Johnson, P. *J. Chem. Phys.* **1993**, *99*, 2322, and references therein.

(24) (a) Innes, K. K.; Byrne, J. P.; Ross, I. G. *J. Mol. Spectrosc.* **1967**, *22*, 125. (b) Gleiter, R.; Heilbronner, E.; Hornung, V. *Helv. Chim. Acta.* **1972**, *55*, 255. (c) Udagawa, Y.; Ito, M.; Suzuka, I. *Chem. Phys. Lett.* **1978**, *60*, 25; *Chem. Phys.* **1980**, *46*, 237. (d) Tomer, J. L.; Holtzclaw, K.; Pratt, D. *J. Chem. Phys.* **1988**, *88*, 1528.

(25) Wenthold, P. G.; Wierschke, S. G.; Nash, J. J., Squires, R. R. *J. Am. Chem. Soc.* **1993**, *115*, 12611; **1994**, *116*, 7378.

(26) Ziegler, T. *Chem. Rev.*, **1991**, *91*, 651.

(27) (a) Binkley, J. S.; Pople, J. A.; Hehre, W. J. *J. Am. Chem. Soc.* **1980**, *102*, 939. (b) Hehre, W. J.; Ditchfield, R.; Pople, J. A. *J. Chem. Phys.* **1972**, *56*, 2257. (c) Krishnan, R.; Frisch, M. J.; Pople, J. A. *J. Chem. Phys.* **1980**, *72*, 4244.

The good performance of MCSCF(n,m)/3-21G procedures that include the full valence π space in geometry optimizations involving unsaturated monoradicals, (π,π)-, (σ,σ)-, and (σ,π)-biradicals as well as closed-shell molecules has been noted previously.[10k,25,28] Geometries obtained by these methods are generally in good agreement with experimental geometries and with geometries derived from MCSCF and coupled-cluster approaches using larger basis sets.[10m,n] Reoptimization of the geometries of **1a**, **2a**, and **3a** using the MCSCF(9,8)/3-21G procedure and the same (low) symmetry constraints as before leads to a higher-symmetry C_{2v} structure for **1a** corresponding to the $^2B_2$ electronic state but still gives localized, low-symmetry structures for **2a** and **3a** corresponding to the $^2A'$ and $^2A_1$ electronic states, respectively. The same structure and total energy for the $^2B_2$ electronic state of **1a** are obtained with and without C_{2v} symmetry constraints. In contrast, imposition of C_{2v} and D_{2h} symmetry constaints on the MCSCF(9,8)/3-21G geometry optimizations for **2a** and **3a** leads to the delocalized $^2B_2$ and ^2A_g electronic states, respectively, but with *higher* total energies compared to the corresponding low-symmetry structures. This energy ordering for the high- and low-symmetry forms of **2a** and **3a** persisted in some, but not all, of the higher level calculations (*vide infra*). The geometries of the $^2A_1$ excited electronic states of **1a** and **2a** and the $^2B_{1u}$ excited electronic state of **3a** were also optimized within C_{2v}, C_{2v}, and D_{2h} symmetries, respectively, at the MCSCF(9,8)/3-21G level. Each of the three electronic states located for **2a** and **3a** and the two electronic states located for **1a** were determined to be true minima by the absence of any negative eigenvalues in the hessian matrices obtained from MCSCF(9,8)/3-21G frequency calculations using numerically-evaluated gradients. The C_{2v} structure of phenyl anion ($^1A_1$) was optimized at the MCSCF-(8,7)/3-21G level, where the active space included the nonbonding σ orbital and all π and π^* orbitals. Optimized geometries for benzene, phenyl radical and the singlet ground states of the neutral benzynes, **1**−**3**, obtained at analogous MCSCF(n,m)/3-21G levels of theory have been reported previously.[10k]

Optimized geometries for the low-lying electronic states of the benzyne anions were also obtained with a hybrid DFT/HF procedure (B3LYP) using the Dunning correlation-consistent, polarized valence double-ζ basis set[29,30] (including six d functions for carbon, designated cc-pVDZ). The B3LYP method employs the Becke three-parameter fit to the combined Hartree−Fock and local density approximations for the exchange energy,[31] and the nonlocal correlation functional given by Lee, Yang, and Parr[32] along with the local correlation functional for the homogeneous electron gas. This functional has performed well in previous calculations of the structures, energies, and vibrational frequencies of both closed- and open-shell molecules,[33] and DFT-based methods are generally noted for giving optimized wave functions for open-shell species with little or no spin contamination.[34] In contrast to the MCSCF results, the B3LYP/cc-pVDZ optimizations give only the higher symmetry, delocalized forms for all three benzyne anions. That is, C_s and C_{2v} stationary points corresponding to the $^2A'$ electronic state of **2a** and the $^2A_1$ electronic state of **3a**, respectively, could not be found by this method. For example, geometry optimization for **3a** starting with the C_{2v} structure for the $^2A_1$ electronic state given by the MCSCF(9,8)/3-21G calculation leads to the same D_{2h} geometry and total energy as are obtained by optimizing with D_{2h} symmetry constraints starting with the MCSCF-derived D_{2h} geometry. Analogous results are obtained in the B3LYP/cc-pVDZ calculations with **2a**: the same C_{2v} structure and total energy are obtained irrespective of the starting geometry and symmetry constraints in the optimization (C_s or C_{2v}). The spin contamination in the DFT-derived wave functions for the benzyne anions is negligible ($<S^2> = 0.755-0.758$). The harmonic frequencies calculated for the optimized, high-symmetry structures of **1a**, **2a**, and **3a** at the B3LYP/cc-pVDZ level are all real, indicating that each structure is a minimum on the global potential energy surface. Attempts to locate the higher energy delocalized electronic states of the three benzyne anions ($^2A_1$ for **1a** and **2a**; $^2B_{1u}$ for **3a**) at the B3LYP/cc-pVDZ level were unsuccessful, as collapse of the wave function to the lower energy configuration consistently occurred during the geometry optimizations.

Tests for the existence of nonplanar structures were carried out at the B3LYP/cc-pVDZ level, since the choice of an appropriate limited active orbital space for an MCSCF calculation on a nonplanar structure is somewhat arbitrary. Optimization of the geometry of **3a** with C_s symmetry constraints (with the symmetry plane passing through the two dehydrocarbons, perpendicular to the heavy atom pseudoplane) and a slightly puckered (chair-like) initial geometry gives a final structure and energy that are identical to those obtained from the full D_{2h} symmetry-constrained calculation which produces the ^2A_g electronic state. Analogous results are obtained from calculations on **1a** and **2a** with C_s symmetry constraints and nonplanar starting geometries: optimization leads to the planar, C_{2v} $^2B_2$ electronic states. Thus, out-of-plane distortion of the benzyne anions is insignificant, at least at the B3LYP/cc-pVDZ level of theory.

Optimized geometries for phenyl anion (C_{2v}), phenyl radical (C_{2v}), and benzene (D_{6h}) were also computed using the B3LYP/cc-pVDZ procedure. Due to the restricted (single-configuration) nature of DFT calculations, no attempts were made to obtain geometries or energies for the singlet states of the neutral benzynes using this method. Selected geometrical parameters for the optimized structures of each of the ions and molecules described above are summarized in Table 1; the atom numbering and angle definitions are shown below. Complete geometry specifications and listings of the unscaled harmonic frequencies obtained at both the MCSCF(n,m)/3-21G and B3LYP/cc-pVDZ levels are available as supporting information.[35]

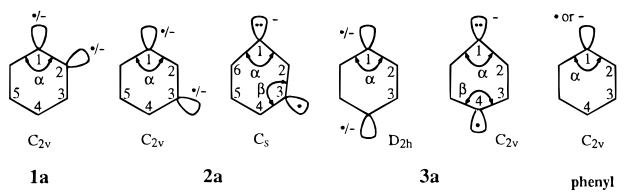

(28) (a) Nachtigall, P.; Jordan, K. J. *J. Am. Chem. Soc.* **1992**, *114*, 4743. (b) Nachtigall, P.; Dowd, P.; Jordan, K. J. *J. Am. Chem. Soc.* **1992**, *114*, 4747. (c) Nash, J. J.; Dowd, P.; Jordan, K. D. *J. Am. Chem. Soc.* **1992**, *114*, 10071. (d) Nachtigall, P.; Jordan, K. D. *J. Am. Chem. Soc.* **1993**, *115*, 270.

(29) Dunning, T. H. *J. Chem. Phys.* **1989**, *90*, 1007.

(30) (a) Dunning, T. H. *J. Chem. Phys.* **1970**, *53*, 2823. (b) Dunning, T. H. *J. Chem. Phys.* **1971**, *55*, 716.

(31) Becke, A. D. *J. Chem. Phys.* **1988**, *88*, 2547.

(32) Lee, C.; Yang, W.; Parr, R. G. *Phys. Rev.* **1988**, *B37*, 785.

(33) (a) Gill, P. M. W.; Johnson, B. G.; Pople, J. A. *Chem. Phys. Lett.* **1992**, *197*, 499. (b) Barone, V. *J. Chem. Phys.* **1994**, *101*, 6834; Barone, V. *Chem. Phys. Lett.* **1994**, *226*, 392. (c) Goldberg, N.; Fiedler, A.; Flammang, R.; Schwarz, H. *Helv. Chim. Acta* **1994**, *77*, 2354.

(34) Baker, J.; Scheiner, A.; Andzelm, J. *Chem. Phys. Lett.* **1993**, *216*, 380.

(35) Ordering information is given on any current masthead page.

Table 1. Selected Geometrical Parameters for **1a**−**3a**, Phenyl Anion, Phenyl Radical and Benzene Obtained from MCSCF(n,m)/3-21G and B3LYP/cc-pVDZ Optimizations[a]

molecule	state, symmetry	method	C_1-C_2	C_2-C_3	C_3-C_4	C_4-C_5	C_5-C_6	C_6-C_1	C*−C* [b]	α	β
1a	$^2B_2$, C_{2v}	MCSCF(9,8)/3-21G	1.351	1.412	1.400	1.405			1.351	120.9	
		B3LYP/cc-pVDZ	1.357	1.404	1.411	1.401			1.357	120.9	
	$^2A_1$, C_{2v}	MCSCF(9,8)/3-21G	1.585	1.413	1.401	1.390			1.585	114.7	
2a	$^2B_2$, C_{2v}	MCSCF(9,8)/3-21G	1.413	1.413	1.407	1.399			2.436	119.8	
		B3LYP/cc-pVDZ	1.411	1.411	1.400	1.405			2.432	119.9	
	$^2A'$, C_s	MCSCF(9,8)/3-21G	1.436	1.393	1.392	1.401	1.399	1.426	2.454	114.5	123.5
	$^2A_1$, C_{2v}	MCSCF(9,8)/3-21G	1.401	1.401	1.413	1.403			2.512	115.3	
3a	^2A_g, D_{2h}	MCSCF(9,8)/3-21G	1.396	1.424					2.900	116.2	
		B3LYP/cc-pVDZ	1.390	1.435					2.908	116.0	
	$^2A_1$, C_{2v}	MCSCF(9,8)/3-21G	1.429	1.412	1.385				2.886	111.8	121.9
	$^2B_{1u}$, D_{2h}	MCSCF(9,8)/3-21G	1.422	1.381					2.835	118.6	
$C_6H_5^-$	$^1A_1$, C_{2v}	MCSCF(8,7)/3-21G	1.435	1.400	1.397					111.0	
		B3LYP/cc-pVDZ	1.426	1.405	1.401					110.7	
C_6H_5	$^2B_1$, C_{2v}	MCSCF(7,7)/3-21G	1.384	1.400	1.398						
		B3LYP/cc-pVDZ	1.380	1.406	1.399					125.8	
C_6H_6	$^1A_1$, D_{6h}	MCSCF(6,6)/3-21G	1.395							120.0	
		B3LYP/cc-pVDZ	1.398							120.0	

[a] Bond distances in Å, bond angles in deg; see text for atom numbering and angle definitions. [b] Distance between the dehydrocarbon atoms.

Table 2. Harmonic Frequencies and Force Constants for Symmetric and Asymmetric Ring Deformation Modes in Benzyne Anions **1a**−**3a** and Neutral Benzyne Triplets **1**−**3**[a]

	ortho		*meta*		*para*	
	1a $^2B_2$	**1** $^3B_2$	**2a** $^2B_2$	**2** $^3B_2$	**3a** ^2A_g	**3** $^3B_{1u}$
ν, cm^{-1}	455 (b_2)	598 (b_2)	482 (b_2)	600 (b_2)	641 (b_{1u})	946 (b_{1u})
	622 (a_1)	583 (a_1)	606 (a_1)	610 (a_1)	632 (a_g)	617 (a_g)
k, mdyn/Å	1.18 (b_2)	1.59 (b_2)	1.12 (b_2)	1.57 (b_2)	1.63 (b_{1u})	3.54 (b_{1u})
	1.57 (a_1)	1.41 (a_1)	1.57 (a_1)	1.51 (a_1)	1.81 (a_g)	1.74 (a_g)

[a] B3LYP/cc-pVDZ vibrational analysis using analytically-evaluated gradients. See text for descriptions of symmetric and asymmetric deformation modes.

Values of the harmonic frequencies and force constants obtained at the B3LYP level for the vibrational modes involved in the molecular distortions in **1a**−**3a** are listed in Table 2, along with the frequencies and force constants for the corresponding modes in the *triplet* states of the neutral benzynes **1**−**3**.[36] A schematic illustration of the normal coordinate displacement vectors for the symmetric (a_1 and a_g) and asymmetric (b_2 and b_{1u}) modes in these species is given in Figure 4. The average zero-point energies of the a and b modes, scaled by a factor of 0.972,[39] are 0.7, 0.8, and 0.9 kcal/mol for **1a**, **2a**, and **3a**, respectively, and 0.8, 0.8, and 1.1 kcal/mol for the triplet states of **1**, **2**, and **3**, respectively.

Energies. Higher-level calculations were carried out for selected electronic states of each of the benzyne anions **1a**−**3a** as well as for the ground electronic states of the benzynes **1**−**3**, benzene, phenyl radical, and phenyl anion, using the MCSCF-derived geometries. Total energies were computed using MCSCF(n,m) procedures with the 6-31G(d) basis set and a modified cc-pVDZ basis set[30] in which the polarization functions on hydrogen atoms were omitted. For the two lowest states of **3a**, the Dunning correlation-consistent polarized valence triple-ζ [10s5p2d1f/4s3p2d1f] basis set for carbon (including six d-functions and ten f-functions) and hydrogen [5s2p1d/3s2p1d] was also used (designated cc-pVTZ).[29] Total energies for each of these species were also computed with the CISD and CASPT2N[37] methods, using the modified cc-pVDZ basis set. The CISD calculations used the optimized natural molecular orbitals resolved from the appropriate MCSCF(n,m)/cc-pVDZ calculations. All symmetry-allowed single and double excitations from a single reference configuration were included (two reference configurations for the singlet benzynes) except those involving the nonvalence molecular orbitals (frozen-core approximation). A Davidson-type correction (DV2) was applied to all CISD energies to account for the effects of quadruple excitations.[38] The CASPT2N energies were derived by applying second-order perturbation theory (MP2) in conjunction with the optimized canonical molecular orbitals obtained from MCSCF-(n,m)/cc-pVDZ calculations. Quadratic CI calculations, including single-, double-, and perturbatively-estimated triple excitations, QCISD(T), were carried out for the $^2B_2$ state of **1a**, the two lowest energy states of **2a** and **3a**, benzene, phenyl radical, and phenyl anion using the modified cc-pVDZ basis set. A few of these calculations were repeated using the analogous coupled-cluster method, CCSD(T). Finally, B3LYP calculations using the cc-pVTZ basis set and the B3LYP/cc-pVDZ derived geometries were carried out for **1a**−**3a**, benzene, phenyl radical, and phenyl anion.

Table 3 gives a listing of the total energy obtained for each of the electronic states of **1a**, **2a**, and **3a** at the indicated level, along with the zero-point vibrational energy (ZPE) and 0−298 K integrated heat capacity ($H_{298} - H_o$) for each species computed from the scaled vibrational frequencies.[39] The 298 K enthalpy of each state relative to the $^2B_2$ ground state of **1a** is given below each total energy. Table 4 presents an analogous listing for **1**−**3**, benzene, phenyl radical, and phenyl anion.

As discussed in the Introduction, artifactual symmetry breaking can produce discontinuities on the potential energy surfaces at the symmetrical minima. Tests for energy cusps were conducted by calculating the total energy for the C_{2v} geometry of **2a** and the D_{2h} geometry of **3a** at different levels of theory with the *orbital symmetry* constraints relaxed to C_s (this can be

(36) Optimized geometries, energies, and unscaled vibrational frequencies for the triplet states of *o*-, *m*-, and *p*-benzyne obtained with the B3LYP/cc-pVDZ procedure are available with the supplemental material.

(37) Andersson, K.; Malmqvist, P.-A.; Roos, B. O. *J. Chem. Phys.* **1992**, *96*, 1218.

(38) (a) Langhoff, S. R.; Davidson, E. R. *Int. J. Quantum Chem.* **1974**, *8*, 61. (b) Blomberg, M. R. A.; Siegbahn, P. E. M. *J. Chem. Phys.* **1983**, *78*, 5682.

(39) The numerically-evaluated frequencies obtained from the MCSCF-(n,m)/3-21G calculations were scaled by a factor of 0.8894, as determined by comparing the experimental zero point vibrational energy for benzene (61.2 kcal/mol) with the value computed from the MCSCF(6,6)/3-21G-derived frequencies (68.8 kcal/mol). The analytically-evaluated frequencies obtained from B3LYP/cc-pVDZ calculations were scaled by a factor of 0.9715, which is similar to the factor recommended by Radom for B3LYP/6-31G* derived frequencies (Radom, L. personal communication of unpublished results).

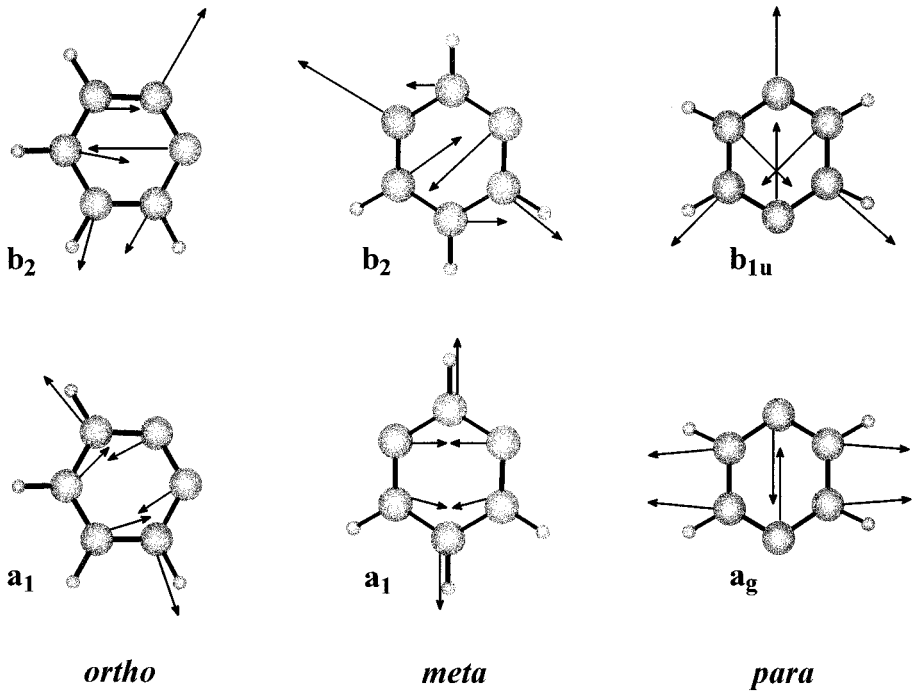

Figure 4. Carbon atom normal coordinate displacement vectors for the component vibrational modes involved in the molecular distortions for *o*-, *m*- and *p*-benzyne anions, **1a**−**3a**.

Table 3. Total Energies (au) and Relative 298 K Enthalpies (kcal/mol) for Benzyne Anions

	ortho **1a**		*meta* **2a**			*para* **3a**		
level[a]	$^2B_2$ C_{2v}	$^2A_1$ C_{2v}	$^2A'$ C_s	$^2B_2$ C_{2v}	$^2A_1$ C_{2v}	$^2A_1$ C_{2v}	^2A_g D_{2h}	$^2B_{1u}$ D_{2h}
MCSCF(9,8)/3-21G	−228.183 29	−228.110 16	−228.169 53	−228.168 40	−228.114 71	−228.161 88	−228.153 87	−228.130 15
	0.0	44.9	7.9	9.7	43.4	13.5	18.7	33.7
MCSCF(9,8)/6-31G(d)	−229.462 66	−229.391 44	−229.450 91	−229.449 36	−229.395 05	−229.444 14	−229.433 96	−229.412 21
	0.0	43.9	6.6	8.7	42.7	11.7	18.2	32.0
MCSCF(9,8)/cc-pVDZ	−229.486 22	−229.415 41	−229.474 86	−229.473 11	−229.419 42	−229.468 57	−229.458 05	−229.435 72
	0.0	43.4	6.4	8.6	42.2	11.2	17.9	32.0
MCSCF(9,8)/cc-pVTZ						−229.509 95	−229.498 49	
						(0.0)	(7.2)	
CISD+DV2/cc-pVDZ	−230.181 19	−230.109 24	−230.169 46	−230.169 00	−230.112 92	−230.161 90	−230.156 21	−230.123 07
	0.0	44.2	6.6	8.0	43.2	12.2	15.9	36.8
QCISD(T)/cc-pVDZ	−230.268 19		−230.257 58	−230.258 88		−230.247 75	−230.251 53	
	0.0		5.9	6.2		12.9	10.7	
CCSD(T)/cc-pVDZ	−230.267 41					−230.245 72	−230.250 65	
	0.0					13.7	10.7	
CASPT2N/cc-pVDZ	−230.198 76	−230.130 52	−230.185 76	−230.193 44	−230.143 44	−230.171 68	−230.185 94	−230.153 22
	0.0	41.8	7.4	3.7	35.0	17.1	8.2	28.9
B3LYP/cc-pVDZ[b]	−230.945 55			−230.937 79			−230.929 08	
	0.0			4.5			9.6	
B3LYP/cc-pVTZ[b]	−230.946 96			−230.936 24			−230.927 18	
	0.0			6.4			11.6	
ZPE[c]	44.9,44.3	43.8	44.0	45.2,44.0	45.2	44.9	45.1,43.5	45.2
$H_{298} - H_o$[c]	3.2,3.4	3.3	3.3	3.2,3.4	3.2	3.2	3.2,3.4	3.2
H_{rel}(298), exptl[d]	0.0			8.7 ± 4.4			15.3 ± 4.2	

[a] The geometry obtained at the MCSCF(n,m)/3-21G level was used unless otherwise noted. [b] Geometry optimized at the B3LYP/cc-pVDZ level. [c] Zero-point vibrational energy and temperature correction, in kcal/mol, determined from harmonic frequencies obtained at the MCSCF(n,m)/3-21G level scaled by a factor of 0.8894. The second number is the corresponding value determined from the harmonic frequencies obtained at the B3LYP/cc-pVDZ level scaled by a factor of 0.9715. [d] Relative enthalpies, in kcal/mol, of isomeric benzyne anions determined from the experimental heats of formation given in ref 1.

done by simply changing one of the off-axis C−H bond lengths by 0.001 Å). A discontinuity is indicated if the energy changes by more than *ca.* 0.1 kcal/mol. The results of tests carried out at the MCSCF(9,8)/3-21G, MCSCF(9,8)/cc-pVDZ, and CISD/cc-pVDZ levels of theory are summarized in Table 5 and will be discussed in a later section.

In order to make direct comparisons between the theoretical results and the experimental thermochemistry, we have derived relative electron, proton, and hydrogen atom-binding energies for selected states of each benzyne anion from the calculated energy changes for the reactions shown below (eqs 2 and 3).

$$C_6H_4\ (\mathbf{1}, \mathbf{2}, \text{or } \mathbf{3}) + C_6H_5^- \xrightarrow{\Delta E} C_6H_4^{\bullet -}\ (\mathbf{1a}, \mathbf{2a}, \text{or } \mathbf{3a}) + C_6H_5 \quad (2)$$

$$C_6H_4^{\bullet -}\ (\mathbf{1a}, \mathbf{2a}, \text{or } \mathbf{3a}) + C_6H_6 \xrightarrow{\Delta E} C_6H_5^- + C_6H_5 \quad (3)$$

By combining the calculated values for $\Delta E(2)$ at 0 K with the

Table 4. Total Energies (au) for *o*-, *m*- and *p*-Benzyne, Benzene, Phenyl Radical, and Phenyl Anion

level[a]	$^1A_1$ *o*-benzyne	$^1A_1$ *m*-benzyne	^1A_g *p*-benzyne	$^1A_1$ benzene	$^2A_1$ phenyl radical	$^1A_1$ phenyl anion
MCSCF(9,8)/3-21G	−228.248 96	−228.216 60	−228.203 98	−229.494 19	−228.846 95	−228.804 59
MCSCF(9,8)/cc-pVDZ	−229.539 55	−229.512 95	−229.495 07	−230.789 11	−230.140 40	−230.112 75
CISD+DV2/cc-pVDZ	−230.194 85	−230.173 38	−230.153 93	−231.497 17	−230.823 75	−230.829 61
QCISD(T)/cc-pVDZ				−231.589 18	−230.904 87	−230.922 79
CASPT2N/cc-pVDZ	−230.201 48	−230.184 14	−230.166 80	−231.497 15	−230.829 00	−230.834 22
B3LYP/cc-pVDZ[b]				−232.267 44	−231.580 56	−231.601 28
B3LYP/cc-pVTZ[b]				−232.234 21	−231.560 21	−231.586 27
ZPE[c]	46.0	46.1	46.0	61.2,61.2	53.7,53.1	52.2,51.6
$H_{298} - H_o$[c]	3.2	3.2	3.2	3.4,3.4	3.3,3.4	3.3,3.4

[a] The geometry obtained at the MCSCF(n,m)/3-21G level was used unless otherwise noted. [b] Geometry optimized at the B3LYP/cc-pVDZ level. [c] Zero-point vibrational energy and temperature correction, in kcal/mol, determined from harmonic frequencies obtained at the MCSCF(n,m)/3-21G level scaled by a factor of 0.8894. The second number is the corresponding value determined from the harmonic frequencies obtained at the B3LYP/cc-pVDZ level scaled by a factor of 0.9715.

Table 5. Effects of Electronic Symmetry-Breaking on the Total Energies of *m*- and *p*-Benzyne Anions Obtained from MCSCF and CISD Calculations[a]

	2a, C_{2v} geometry			**3a**, D_{2h} geometry		
level	$^2B_2$ (C_{2v})	$^2A'$ (C_s)	ΔE	^2A_g (D_{2h})	$^2A'$ (C_s)	ΔE
MCSCF(9,8)/3-21G	−228.168 40	−228.168 40	0.0	−228.153 87	−228.155 90	1.3
MCSCF(9,8)/cc-pVDZ	−229.473 11	−229.473 12	0.0	−229.458 05	−229.461 96	2.5
CISD/cc-pVDZ	−230.030 33	−230.030 33	0.0	−229.013 76	−229.023 42	6.1
CISD+DV2/cc-pVDZ	−230.169 00	−230.169 02	0.0	−229.156 21	−229.155 54	−0.4

[a] Total energies (au) calculated for each ion with the indicated orbital symmetry constraint; the energy differences are given in kcal/mol.

Table 6. Relative and Absolute Electron Binding Energies of Benzyne Anions (kcal/mol)[a]

	ortho **1a**		*meta* **2a**			*para* **3a**		
level[b]	$^2B_2$ C_{2v}	$^2A_1$ C_{2v}	$^2A'$ C_s	$^2B_2$ C_{2v}	$^2A_1$ C_{2v}	$^2A_1$ C_{2v}	^2A_g D_{2h}	$^2B_{1u}$ D_{2h}
MCSCF(9,8)/3-21G	15.0	59.8	2.4	4.3	37.9	0.24	5.4	20.4
	10.3	−34.5	22.9	21.0	−12.7	25.0	19.9	4.9
MCSCF(9,8)/cc-pVDZ	16.5	59.8	6.0	8.2	41.9	−0.32	6.4	20.5
	8.8	−34.5	19.3	17.0	−16.7	25.6	18.9	4.7
CISD+DV2/cc-pVDZ	12.6	56.7	5.6	7.0	42.2	−0.92	2.8	23.7
	12.7	−31.4	19.7	18.3	−16.9	26.2	22.5	1.6
CASPT2N/cc-pVDZ	5.3	47.1	1.7	−2.0	29.4	0.61	−8.2	12.4
	19.9	−21.8	23.6	27.2	−4.1	24.7	33.5	12.9
exptl	12.4 ± 0.2			5.8 ± 0.3			-3.5 ± 0.5	
	12.9 ± 0.2			19.5 ± 0.3			28.8 ± 0.5	

[a] Top number is the calculated energy change at 0 K for the electron transfer reaction shown in eq 2; bottom number is the absolute electron binding energy derived for each state. [b] Geometries obtained at the MCSCF(n,m)/3-21G level.

experimental electron affinity of phenyl radical ($EA(C_6H_5) = 25.3 \pm 0.1$ kcal/mol[22]), estimates of the absolute electron binding energies of each benzyne anion state can be derived. The relative and absolute electron binding energies obtained in this way from the different levels of theory are listed in Table 6, along with the experimentally-determined electron affinities for each of the benzynes. The calculated enthalpy changes at 298 K for eq 3 can be combined with the well-established experimental values for the gas-phase acidity of benzene ($\Delta H_{acid}(C_6H_6 = 401.7 \pm 0.5$ kcal/mol[40]) and the C−H bond dissociation enthalpy of benzene ($DH_{298}[C_6H_5\text{-}H] = 113.5 \pm 0.5$ kcal/mol[40]) in order to derive the acidities of phenyl radical in the *ortho*, *meta* and *para* positions, and the corresponding C−H bond strengths in phenyl anion. Values for $\Delta H(3)$ and the derived acidities and bond enthalpies obtained at several different levels of theory are presented in Table 7.

The geometry optimizations, vibrational frequency calculations, QCISD(T), CCSD(T), and density-functional theory calculations were performed with the GAUSSIAN 92/DFT program, Revision G.3.[41] The MCSCF, CISD, and CASPT2N single-point calculations were performed with MOLCAS[42] versions 2 and 3.

Discussion

Structures of Benzyne Anions. The optimized geometries obtained with the MCSCF(9,8)/3-21G and B3LYP/cc-pVDZ procedures for the $^2B_2$ electronic states of **1a** and **2a** and the ^2A_g electronic state of **3a** are essentially the same. The largest deviation between bond distances computed by either method is only 0.011 Å. The geometries of the two high-symmetry, delocalized forms of **1a**, **2a**, and **3a** can be compared with the optimized geometries obtained from analogous MCSCF calculations for the corresponding neutral benzynes, which can be found in Table 1 of reference 10k. Increased electron−electron repulsion accompanying addition of a third electron to the two valence σ orbitals of a neutral benzyne generally leads to expanded CC bond distances and decreased CCC angles about the dehydrocarbons. Compared to the singlet benzynes, the distances between the dehydrocarbons (C*−C* in Table 1) in

(40) Davico, G. E.; Bierbaum, V. M.; DePuy, C. H.; Ellison, G. B.; Squires, R. R. *J. Am. Chem. Soc.* **1995**, *117*, 2590.

(41) Frisch, M. J.; Trucks, G. W.; Schlegel, H. B.; Gill, P. M. W.; Johnson, B. G.; Wong, M. W.; Foresman, J. B.; Robb, M. A.; Head-Gordon, M.; Replogle, E. S.; Gomperts, R.; Andres, J. L.; Raghavachari, K.; Binkley, J. S.; Gonzalez, C.; Martin, R. L.; Fox, D. J.; DeFrees, D. J.; Baker, J.; Stewart, J. J. P.; Pople, J. A. Gaussian, Inc.: Pittsburgh, PA, 1993.

(42) Andersson, K.; Blomberg, M. R. A.; Fülscher, M. P.; Kellö, V.; Lindh, R.; Mamlqvist, P. -A.; Noga, J.; Olsen, J.; Roos, B. O.; Sadlej, A. J.; Siegbahn, P. E. M.; Urban, M.; Widmark, P.-O. University of Lund, Sweden, 1992, 1994.

Table 7. Relative and Absolute Proton and Hydrogen Atom Affinities of Benzyne Anions (kcal/mol)[a]

	ortho **1a**	*meta* **2a**		*para* **3a**	
level[b]	$^2B_2$ C_{2v}	$^2A'$ C_s	$^2B_2$ C_{2v}	$^2A_1$ C_{2v}	^2A_g D_{2h}
MCSCF(9,8)/3-21G	16.2	8.3	6.5	2.6	−2.5
	385.6	393.5	395.3	399.1	404.2
	97.4	105.3	107.1	110.9	116.0
MCSCF(9,8)/cc-pVDZ	13.8	7.4	5.2	2.6	−4.1
	388.2	394.3	396.5	399.1	405.8
	100.0	106.1	108.3	110.9	117.6
CISD+DV2/cc-pVDZ	15.6	8.9	7.6	3.4	−0.32
	386.1	392.8	394.1	398.4	402.0
	97.9	104.6	105.9	110.2	113.8
QCISD(T)/cc-pVDZ	18.5	12.6	12.3	5.6	7.9
	383.2	389.1	389.4	396.1	393.8
	95.0	100.9	101.2	107.9	105.6
CASPT2N/cc-pVDZ	20.4	13.0	16.7	3.3	12.1
	381.3	388.7	385.0	398.4	389.6
	93.1	100.5	96.8	110.2	101.3
B3LYP/cc-pVDZ[c]	18.8	14.3		9.3	
	382.9	387.4		392.4	
	94.7	99.2		104.2	
B3LYP/cc-pVTZ[c]	21.1	14.7		9.4	
	380.6	387.0		392.3	
	92.4	98.8		104.1	
exptl ΔH(3)	23.5 ± 3.1	14.8 ± 3.1		8.2 ± 2.9	
$\Delta H_{acid}(C_6H_5)$	378.2 ± 3.1	386.9 ± 3.1		393.5 ± 2.9	
$DH_{298}[C_6H_4^-$-H]	90.1 ± 3.1	98.8 ± 3.1		105.4 ± 2.9	

[a] The top number is the calculated enthalpy change at 298 K for the reaction shown in eq 3; the second and third numbers are the gas-phase acidity of phenyl radical and the C−H bond dissociation enthalpy of phenyl anion at the corresponding ring positions. [b] The geometry obtained at the MCSCF(n,m)/3-21G level was used unless otherwise noted. [c] Geometry optimized at the B3LYP/cc-pVDZ level.

the lower-energy, high-symmetry forms of the radical anions increase by 7−8%. Because the antibonding combination orbital (Ψ_-) is doubly-occupied in the higher energy $^2A_1$ electronic states of **1a** and **2a**, the relative increases are larger: *ca.* 26% for **1a** and 12% for **2a**. In the $^2B_2$ electronic state of **1a**, the distance between the dehydrocarbons (1.35 Å) is intermediate between those of the singlet and triplet states of neutral *o*-benzyne **1** (1.26 and 1.41 Å, respectively). This order of bond distances is typical for vicinal π systems because there is residual π-bonding in the radical anion, while the π-antibonding character dominates in the triplet state of the neutral molecule. The structural manifestations of through-bond coupling[9] (Ψ_- mixing with the C_2-C_3 and C_5-C_6 σ^* orbitals) are clearly evident in the geometries computed for the ^2A_g and $^2B_{1u}$ electronic states of **3a**. As with the singlet and triplet states of *p*-benzyne (**3**), the distance between the dehydrocarbons is slightly smaller (*ca.* 0.06 Å) in the higher energy electronic state since the intervening bonds (C_2-C_3 and C_5-C_6) are shorter. However, the *difference* in CC bond length alternation is much more pronounced in the radical anion since the through-bond coupling interaction involves a two-electron stabilization in the ^2A_g configuration but only a one-electron stabilization in the $^2B_{1u}$ configuration.

The low-symmetry electronic states of **2a** ($^2A'$) and **3a** ($^2A_1$) have essentially the same distances between the dehydrocarbons as in the corresponding $^2B_2$ and ^2A_g electronic states but markedly different CCC bond angles about each of the two dehydrocarbons. The low-symmetry structures for **2a** and **3a** are both clearly hybrids of a phenyl radical and a phenyl anion, with long CC bonds and a small angle about one dehydrocarbon and short CC bonds and a large angle about the other. These bond length and bond angle changes relative to benzene can be understood in terms of the varying s-character in the CC bonds about the dehydrocarbons. In phenyl anion, s-character is diminished in the CC bonds so it can be maximized in the lone-pair orbital. The greater length and higher p-character of the bonds naturally leads to a smaller CCC angle. In phenyl radical s-character is somewhat enhanced in the CC bonds at the expense of the nonbonding orbital since the latter is only singly-occupied. Short CC bonds and a larger CCC angle naturally result.

The absence of a localized, C_s symmetry ($^2A'$) minimum for *o*-benzyne anion **1a** in the unconstrained MCSCF geometry optimization can be understood in terms of the much larger $|\Psi_- - \Psi_+|$ orbital energy gap in this ion compared to those in **2a** and **3a** and the diminished pseudo Jahn-Teller interaction that results. At the MCSCF(9,8)/3-21G level, the energy gap between the resolved $10a_1$ (Ψ_+) and $8b_2$ (Ψ_-) canonical orbitals for **1a** is 179 kcal/mol, while for **2a** and **3a** the splittings between the corresponding orbitals are only 111 and 77 kcal/mol, respectively.[43] Therefore, vibronic coupling between the ground state $(a_1)^2(b_2)^1$ and excited state $(a_1)^1(b_2)^2$ configurations in **1a** is evidently too weak to induce distortion, whereas in **2a** and **3a** the smaller splittings permit sufficient mixing for the distortions to occur. In this sense, *m*- and *p*-benzyne anions are analogous to formoxyl radical (HCO_2) and oxirane molecular ion ($CH_2OCH_2^{\bullet+}$). The "allylic resonance" in these two radicals is relatively weak due to the relatively small energy gaps between the π orbitals,[17] and low-symmetry C_s structures with two different CO bond distances are essentially degenerate with high-symmetry C_{2v} structures.[18] In contrast, the *o*-benzyne anion is more like allyl radical (CH_2CHCH_2), wherein the π orbital splittings are larger and the C_{2v} minimum is much more rigid.

Electronic State Energies, Symmetry-Breaking, and Vibronic Coupling. The MCSCF(9,8) and CISD+DV2 calculations predict the same electronic state orderings and relative enthalpies for the three benzyne anions. The $^2A_1$ electronic state of **1a** is computed to lie about 44 kcal/mol above the $^2B_2$ electronic state. For *m*-benzyne anion **2a**, the localized radical anion form, $^2A'$, is predicted to be lowest in energy, lying 1−2 kcal/mol below the delocalized C_{2v} $^2B_2$ electronic state. The $^2A_1$ electronic state is calculated to lie about 36 kcal/mol higher in energy. A similar picture emerges for **3a**: the low-symmetry $^2A_1$ electronic state is predicted to lie 3−7 kcal/mol below the high-symmetry ^2A_g electronic state, and the $^2B_{1u}$ electronic state lies 21−25 kcal/mol higher. The difference in energy between the $^2A_1$ and ^2A_g electronic states of **3a** obtained at the MCSCF(9,8) level with the 6-31G(d), cc-pVDZ, and cc-pVTZ basis sets is essentially the same, suggesting that the MCSCF calculations are converged with respect to basis set size.

However, the predictions of low-symmetry ground states for **2a** and **3a** by the MCSCF and CISD calculations must be viewed with suspicion, since these systems are subject to artifactual symmetry-breaking. In fact, the additional calculations summarized in Table 5 indicate that the computed electronic state ordering for **3a** is an artifact. For example, relaxation of the *orbital* symmetry constraints to C_s in single-point energy calculations at the C_{2v} geometry of **2a** and at the D_{2h} geometry of **3a** at the MCSCF(9,8)/3-21G, MCSCF(9,8)/cc-pVDZ, and CISD/cc-pVDZ levels of theory leads to substantial decreases in the energy of **3a** (1−6 kcal/mol) but no changes in the energies of **2a**. This means that, at these levels of theory, an energy cusp exists at the D_{2h} geometry for **3a** on the symmetry-constrained potential energy surface. Therefore, the distortion

(43) At the ROHF/6-31G* level of theory, these orbital gaps are 116, 80, and 58 kcal/mol, while at the B3LYP/cc-pVDZ level they are 51, 32, and 28 kcal/mol, respectively.

from D_{2h} to C_{2v} symmetry that accompanies the unconstrained MCSCF(9,8)/3-21G geometry optimization is an artifact of the inadequate $\sigma-\pi$ correlation provided by this method. It is noteworthy that inclusion of the estimated effects of quadruple excitations in the CISD calculations (DV2) for **3a** substantially reduces the energy anomaly. This means that the (approximated) quadruple excitations are providing enough additional electron correlation to give about the same CI energy for the two different sets of initial orbitals. In contrast, the total energy of **2a** is independent of any orbital symmetry constraints. This indicates that the MCSCF(9,8)/3-21G surface for **2a** is continuous in the region of the C_{2v} structure and that the distortion to C_s symmetry which occurs in the unconstrained optimization at this level is not an artifact.

The QCISD(T), CCSD(T), CASPT2N, and DFT(B3LYP) calculations tell a different story. For **3a**, the delocalized ^2A_g electronic state is found to be the lowest in energy by all of these methods, and, according to DFT, it is the *only* stationary state. The localized C_{2v} structure for **3a** is predicted to lie higher in energy by 2−3 kcal/mol with the QCISD(T) and CCSD(T) methods. The $^2A_g - {}^2A_1$ energy difference is considerably greater at the CASPT2N level, *ca.* 9 kcal/mol. Comparing the CASPT2N and MCSCF(9,8) energies reveals that this is due to the combined effects of a larger energy decrease for the ^2A_g electronic state (0.728 au) and a smaller energy decrease for the $^2A_1$ electronic state (0.703 au), relative to the differentials for the other benzyne anion states (0.711−0.720 au), which results from the MP2 correction to the MCSCF energies in the CASPT2N calculations. That is, the dynamic electron correlation estimated by the CASPT2N method stabilizes the high-symmetry form and destabilizes the low symmetry form of **3a** to a relatively greater extent.

At the QCISD(T) level, the $^2B_2$ electronic state of **2a** lies slightly lower in energy than the $^2A'$ electronic state. However, the ZPE and temperature corrections reverse this ordering such that the localized form lies about 0.3 kcal/mol below the delocalized form.[44] The CASPT2N calculations predict a larger energy difference favoring the $^2B_2$ electronic state by about 3.7 kcal/mol, which can again be traced to a greater stabilization of the delocalized form by dynamic electron correlation effects. The B3LYP/cc-pVDZ calculations find the delocalized $^2B_2$ electronic state of **2a** to be the only stationary state on the computed potential energy surface. Because the hybrid DFT/HF B3LYP method is nonvariational, the absolute total energies computed for **2a** and **3a** (but not **1a**) actually increase upon expanding the basis set from cc-pVDZ (110 basis functions) to cc-pVTZ (270 basis functions). The B3LYP energies of **2a** and **3a** relative to **1a** increase by about 2 kcal/mol in going to the larger basis set.

The relative enthalpies of the lowest energy states of **1a**−**3a** computed by the different methods are in good agreement: **2a** is predicted to lie 4−6 kcal/mol higher in energy than **1a**, and **3a** is higher in energy than **2a** by another 4−5 kcal/mol. These energy differences are in fair agreement with the experimental estimates, shown at the bottom of Table 3, which were derived in the preceding paper[1] from the measured heats of formation and electron affinities of the neutral benzynes, **1**−**3**. Because of the presence of artifactual symmetry-breaking in the MCSCF and CISD calculations for **3a**, the results derived from the QCISD(T), CASPT2N, and B3LYP calculations are considered to be the most reliable: the delocalized, high-symmetry forms of **1a**−**3a** represent the lowest energy electronic states for these ions. Indeed, since the symmetry-breaking problem was evident in the MCSCF(9,8)/3-21G procedure used to optimize the geometries, any results based on these structures should be regarded with caution. Nevertheless, the close similarities between the structures for the delocalized radical anion forms given by the B3LYP and MCSCF procedures suggests that the errors introduced by using the MCSCF geometries will not be large.

In view of the discrepancies regarding the nature of the lowest energy electronic states for **2a** and **3a** and the differing results of the tests for artifactual symmetry-breaking in the MCSCF and CISD calculations for these two ions, it remains unclear whether the low-symmetry structures represent true energy minima. If the distorted structures are minima, then the real issue is whether or not the barrier between the high- and low-symmetry forms on the global potential energy surface lies above or below the zero-point level for the active vibronic modes (b_2 for **2a**; b_{1u} for **3a**, *vide infra*). If the barrier is lower, then the molecule necessarily exists as a fluxional, dynamically-coupled vibronic state, and the notion of discrete geometric forms is not valid.[45] Only when the barrier is well above this zero-point energy level does it make any sense to think about isomeric forms with distinct structures and reactivity. In fact, the potential energy surfaces in the vicinity of the distorted and nondistorted stationary points located for **2a** and **3a** at the MCSCF(9,8)/3-21G and CISD+DV2/cc-pVDZ levels of theory appear to be quite flat. While rigorous searches for transition states connecting the high- and low-symmetry forms of **2a** and **3a** were not performed, we did calculate total energies for partially-optimized geometries that had fixed CCC angles about the dehydrocarbons, α and β, that were intermediate between the optimized values determined for the high- and low-symmetry forms. In each case the computed energy of the "intermediate" geometry was found to lie below that of the higher energy, higher symmetry form (for **3a** the comparison is made to the energy of the D_{2h} structure obtained with relaxed orbital symmetry). Analogous calculations carried out at the B3LYP/cc-pVDZ level of theory give similar results. The B3LYP/cc-pVDZ energies of the C_s and C_{2v} geometries for **2a** and **3a** obtained from the MCSCF(9,8)/3-21G calculations are only 1.9 and 3.1 kcal/mol, respectively, higher than the optimal energies of the high-symmetry forms, and the computed energies for structures with intermediate values of α and β lie in between the two extremes. Thus, the angular distortions in **2a** and **3a** are associated with small, essentially monotonic energy changes. Since the calculations indicate little or no barrier for these distortions in **2a** and **3a**, we conclude that *m*- and *p*-benzyne anions are fluxional species, with *effectively* high-symmetry structures that undergo zero-point excursions to distonic radical anion forms with reduced molecular symmetry and (relatively) localized odd-spin and charge distributions.

(44) The relative energies of the different electronic states of **1a**, **2a**, and **3a** determined by the various components of the QCISD(T) and CCSD(T) calculations indicate pronounced effects due to spin-contamination, and large stabilizing effects on the delocalized states due to triple substitutions. For example, the UHF wave functions for the $^2A'$ and $^2B_2$ electronic states of **2a** and the $^2A_1$ electronic state of **3a** are extremely spin-contaminated, with $<S^2>$ values around 1.2 (for $^2B_2$ **1a** and ^2A_g **3a**, $<S^2>$ is 0.78). The MPn energies for the delocalized electronic states of **2a** and **3a** are generally lower than those of the localized electronic states, but the differences change in an erratic manner with increasing level of theory. The perturbatively-estimated triple substitutions in the QCISD(T) and CCSD(T) calculations reduce the energies of the delocalized electronic states of **2a** and **3a** by 2.4−3.9 kcal/mol, but increase the energies of the corresponding localized electronic states by 0.2−0.7 kcal/mol.

(45) For a discussion of the notion of molecular "shape" in the context of the Born-Oppenheimer approximation, see: Wooley, R. G. *J. Am. Chem. Soc.* **1978**, *100*, 1073. For a recent example of the experimental description of a molecule without a definite "shape", see: Lindner, R.; Müller-Dethlefs, K.; Wedum, E.; Haber, K.; Grant, E. *Science* **1996**, *271*, 1698.

Specifying the zero-point energies for the highly anharmonic Jahn-Teller modes in **2a** and **3a** is problematic since the calculated harmonic frequencies for the component vibrational modes listed in Table 2 can only give crude upper limits. Moreover, because of artifactual symmetry-breaking in the MCSCF(9,8)/3-21G wave functions, and because the MCSCF-(9,8)/3-21G vibrational frequencies were derived from numerically-evaluated energy gradients, the frequencies for nonsymmetric modes obtained by this method are unreliable.[46] The vibrational frequencies derived from the B3LYP/cc-pVDZ calculations were obtained with analytical gradients and are therefore more reliable. Despite the harmonic approximation, the trends in the frequencies and force constants listed in Table 2 clearly indicate the nature of the vibronic coupling that accompanies addition of an electron to a neutral benzyne. The symmetric ring-angle deformation modes (a_1 and a_g) in the benzyne anions and the neutral triplet benzynes have similar magnitudes of the frequencies (583−632 cm^{-1}) and force constants (1.41−1.81 mdyn/Å). The asymmetric b_2 modes in *o*- and *m*-benzyne triplets are also similar ($\nu_{av} = 599$ cm^{-1}; $k_{av} = 1.58$ mdyn/Å). However the corresponding b_{1u} mode in triplet *p*-benzyne is much "stiffer" ($\nu = 946$ cm^{-1}, $k = 3.54$ mdyn/Å). Addition of an electron to form the benzyne anions results in marked decreases in the frequencies and force constants for the asymmetric deformation modes. The change in the b_{1u} mode in going from **3** to **3a** is especially pronounced, amounting to a 50% reduction in the force constant, and a corresponding drop in the frequency by about a third. Thus, compared to the symmetric modes, the asymmetric ring-angle deformation modes in the neutral benzynes become considerably "softer" upon addition of a third electron to the two valence orbitals as a result of pseudo Jahn-Teller interactions.

Thermochemistry. At most of the levels of theory employed in this study, the benzyne anions are calculated to be unbound, *i.e.*, the total energies of the negative ions are smaller (less negative) than those of the corresponding neutral benzynes. This is a common outcome for calculations on molecular anions using limited basis sets and incomplete electron correlation. However, it has been shown that relative electron affinities derived from electron transfer reactions such as that shown in eq 2 can be quite accurate.[47] The calculated electron binding energies of the lowest energy forms of **1a**−**3a** can be compared with the experimentally-determined electron affinities of the three neutral benzynes. The performance of the MCSCF and CASPT2N methods in predicting both the relative and absolute electron binding energies of **1a**−**3a** is poor in most instances. For example, the EAs for *o*-benzyne and *p*-benzyne are underestimated by the MCSCF procedure, with errors of −3.9 and −3.5 kcal/mol in the calculations using the larger basis set and with −2.6 and −3.8 kcal/mol errors in the calculations using the smaller basis set. For the *meta* isomer, the poor match with the smaller basis set calculation ($\Delta = +3.4$ kcal/mol) is improved with the larger basis set ($\Delta = -0.2$ kcal/mol). The electron binding energies obtained from the CASPT2N procedure are considerably overestimated, with deviations from experiment of +7.0, +7.7, and +4.7 kcal/mol for **1a**, **2a**, and **3a**, respectively. With both the MCSCF and CASPT2N methods, the *ortho*/*meta* difference is overestimated, and the *meta*/*para* difference is underestimated, suggesting that the calculated value for the *meta* isomer is systematically too low. In contrast, the predicted electron binding energies for the ground states of the benzyne anions obtained from the CISD+DV2/cc-pVDZ calculations appear to be in very good agreement with the experimental data, with deviations of −0.2, +0.2, and −2.6 kcal/mol for **1a**, **2a**, and **3a**, respectively. However, the good match is probably fortuitous, since the CISD procedure incorrectly predicts localized ground states for **2a** and **3a**, and the electron binding energies computed for the corresponding delocalized forms show large errors (−2.5 and −9.9 kcal/mol, respectively). Finally, all of the theoretical models employed in this study predict that the $^2A_1$ states of **1a** and **2a** are unbound with respect to electron detachment (EA < 0). In fact, in their photoelectron study of **1a**, Leopold *et al.* did not observe any hot-band activity in the spectrum that could be attributed to excited states of the anion.[48] The $^2B_{1u}$ state of **3a** is predicted to be only weakly bound (EA = 0.1−0.2 eV, neglecting the CASPT2N result). However, the energy of this state is too high (≈30 kcal/mol above the ground state) for it to be populated to any significant extent at room temperature.

The calculated enthalpy changes for eq 3 show considerable variation with the different computational approaches. The computed values from the MCSCF and CISD procedures are much smaller than those obtained from the QCISD(T), CASPT2N, and B3LYP calculations—by nearly a factor of 2 in some cases. With the exception of the CASPT2N results for **3a**, the energetics obtained with the latter three methods are all within the indicated error limits on the experimental values. The large basis set B3LYP calculations perform remarkably well in predicting the measured thermochemistry. Thus, theory and experiment concur that the *ortho*, *meta*, and *para* C−H bonds in phenyl anion are weaker than the C−H bonds in benzene by about 22, 15, and 8 kcal/mol, respectively, and that the corresponding C−H bonds in phenyl radical are more acidic than the C−H bonds in benzene by these same amounts. The origin of these significant homolytic and heterolytic bond strength reductions is the additional delocalization of negative charge and odd-spin density provided by the second open-shell carbon in each benzyne anion.

Concluding Remarks

Based on the experimental and theoretical results for the benzyne anions and the previous studies of the neutral benzynes, we can venture some predictions about the photoelectron spectra that may ultimately be obtained for **2a** and **3a**. The spectrum for **2a** should display relatively sharp, well-resolved features for detachment from the $^2B_2$ ground state of the anion to the $^1A_1$ ground state and the $^3B_2$ excited state of *m*-benzyne at around 0.85 and 1.6 eV, respectively. Prominent vibrational progressions may be evident in the a_1 and b_2 modes of each neutral state due to the significant differences in the geometries and fluxional behavior of the anion and neutral species. The spectrum for **3a** should be quite congested in the region of the lowest energy feature (*ca.* 1.25 eV), with overlapping bands for detachment to the ^1A_g and $^3B_{1u}$ states of **3** that are separated by only about 0.1−0.2 eV. Vibrational structure in each band corresponding to the a_g and b_{1u} modes may also be observable. However, since the (bound) $^2B_{1u}$ excited state of **3a** lies at approximately the same energy as the predicted ($^1A_g \leftarrow {}^2A_g$) transition, autoionization could lead to spectral line broadening.

(46) Frequencies and force constants for any nontotally symmetric vibrational motions obtained from MCSCF calculations that employ numerically- rather than analytically-evaluated energy gradients are invariably too high since any symmetry-breaking nuclear displacement used to evaluate the molecular force field by finite energy differences will eliminate the symmetry-constrained configuration mixings within the active space.

(47) Equation 2 may not actually provide proper cancellation of electron correlation errors and basis set deficiencies since it is not *isogyric*, i.e., the total electron spin is not the same for the products and reactants.

(48) Leopold, D. G.; Miller, A. E. S.; Lineberger, W. C. *J. Am. Chem. Soc.* **1986**, *108*, 1379.

The excellent performance of density functional theory in predicting the thermochemistry of benzyne anions and the absence of artifactual symmetry breaking in the DFT calculations on these species suggest that this level of theory is particularly well-suited for computational studies of distonic radical anions derived from biradicals. Its applicability to relatively large molecules is especially noteworthy. We have already carried out DFT calculations on the radical anions derived from trimethylenemethane and α,3-dehydrotoluene which also show excellent correspondence with the available experimental results. DFT calculations on radical anions derived from a series of non-Kekule hydrocarbons such as 2,4-bismethylenecyclobutane-1,3-diyl and *m*-xylylene are currently in progress.

Acknowledgment. We are grateful to Professors Ed Grant and Wes Borden for many helpful discussions. This work was supported by the National Science Foundation and the Department of Energy, Office of Basic Energy Sciences.

Supporting Information Available: Listings of geometries (in GAUSSIAN Z-matrix format) and harmonic vibrational frequencies for benzyne anions, neutral benzynes, benzene, phenyl anion, and phenyl radical, obtained with MCSCF(n,m)/3-21G and B3LYP/cc-pVDZ procedures (10 pages). See any current masthead page for ordering and Internet access instructions.

JA9606642